

1       Comprehensive transcriptomic analysis shows disturbed calcium  
2               homeostasis and deregulation of T lymphocyte apoptosis in  
3                               inclusion body myositis

4       Mridul Johari<sup>1,2\*</sup>, MSc, Anna Vihola<sup>1,2,3</sup>, PhD, Johanna Palmio<sup>4</sup>, MD, PhD, Manu Jokela<sup>3,5</sup>, MD,  
5       PhD, Per Harald Jonson<sup>1,2</sup>, PhD, Jaakko Sarparanta<sup>1,2</sup>, PhD, Sanna Huovinen<sup>6</sup>, MD, Marco  
6       Savarese<sup>1,2</sup>, PhD, Peter Hackman<sup>1,2</sup>, PhD, Bjarne Udd<sup>1,2,4,7</sup>, MD, PhD

7  
8       <sup>1</sup>Folkhälsan Research Center, Helsinki, Finland

9       <sup>2</sup>Department of Medical Genetics, Medicum, University of Helsinki, Finland

10       <sup>3</sup>Neuromuscular Research Center, Department of Genetics, Fimlab Laboratories, Tampere, Finland

11       <sup>4</sup>Neuromuscular Research Center, Department of Neurology, Tampere University and University Hospital, Tampere,  
12       Finland

13       <sup>5</sup>Division of Clinical Neurosciences, Department of Neurology, Turku University Hospital, Turku, Finland

14       <sup>6</sup>Department of Pathology, Fimlab Laboratories, Tampere University Hospital, Tampere, Finland

15       <sup>7</sup>Department of Neurology, Vaasa Central Hospital, Vaasa, Finland

16  
17  
18

19       \*Corresponding Author

20       Mridul Johari, MSc

21       Folkhälsan Research Center,

22       Department of Medical Genetics, Medicum, University of Helsinki

23       Biomedicum, Haartmaninkatu 8, PO Box 63, FI-00014 Helsinki, Finland

24       Email: [mridul.johari@helsinki.fi](mailto:mridul.johari@helsinki.fi)

25       Tel (office): +358 2941 25629

26  
27  
28  
29

## 30 **Abstract**

31 **Objective:** Inclusion body myositis (IBM) has an unclear molecular etiology due to the co-existence  
32 of characteristic cytotoxic T-cell activity and degeneration of muscle fibers. Using in-depth gene  
33 expression and splicing studies, we aimed at understanding the different components of the molecular  
34 pathomechanisms in IBM.

35 **Methods:** We performed RNA-seq on total RNA extracted from skeletal muscle biopsies of clinically  
36 and histopathologically defined IBM (n=24), tibial muscular dystrophy (n=6), and  
37 histopathologically normal controls (n=9). In a comprehensive transcriptomics analysis, we analyzed  
38 the differential gene expression, differential splicing and exon usage, downstream pathway analysis,  
39 and the interplay between coding and non-coding RNAs (micro RNAs and long non-coding RNAs).

40 **Results:** We observe IBM-specific dysregulation of genes involved in calcium homeostasis,  
41 particularly affecting the T-cell activity and regulation, causing disturbed  $Ca^{2+}$  induced apoptotic  
42 pathway of T cells in IBM muscles. Additionally, LCK/p56, which is an essential gene in regulating  
43 the fate of T-cell apoptosis, shows altered expression and splicing usage in IBM muscles

44 **Interpretation:** Our analysis provides a novel understanding of the molecular mechanisms in IBM by  
45 showing a detailed dysregulation of genes involved in calcium homeostasis and its effect on T-cell  
46 functioning in IBM muscles. Loss of T-cell regulation is hypothesized to be involved in the consistent  
47 observation of no response to immune therapies in IBM patients. Our results show that loss of  
48 apoptotic control of cytotoxic T cells in IBM could indeed be one component of their abnormal  
49 cytolytic activity in IBM muscles.

## 50 **Introduction**

51 Inclusion body myositis (IBM) is a late-onset, acquired muscle disease with unclear etiology, and the  
52 poorly understood molecular pathogenesis is under debate due to several factors. The CD8<sup>+</sup> T-cell  
53 infiltration and overexpression of class I MHC antigens in all muscle fibers indicate an autoimmune  
54 cascade and are, in fact, the most consistent finding together with the degeneration of myofibers.  
55 However, IBM largely remains refractory to immunosuppressive drugs<sup>1</sup>, and comprehensive clinical  
56 trials have generally been ineffective<sup>2</sup>. A partial clinical and histopathological overlap with other  
57 rimmed-vacuolar (RV) myopathies<sup>3</sup>, the occurrence of rare familial cases<sup>4</sup>, and the protein  
58 accumulations in the RVs<sup>5</sup> support a degenerative muscle pathology. Additionally, previous studies  
59 showing a strong genetic association with 8.1 ancestral haplotype<sup>6, 7</sup> support a possible genetic  
60 predisposition for IBM. Accumulation/aggregation of these misfolded proteins suggests that IBM  
61 could be a protein aggregate disease with immune-mediated cytotoxic inflammation as a resulting  
62 secondary feature<sup>8</sup>. However, there is a significant variance in nature and the number of accumulated  
63 proteins observed in the IBM muscle biopsies<sup>9</sup>. Similar aggregates observed in HIV-associated IBM<sup>10</sup>  
64 suggest that protein aggregation can still be a downstream effect of immune dysfunction.

65 Analysis of tissue-specific mRNAs and subsequent RNA-seq based transcriptomics studies focused  
66 on understanding the expression of genes, participating pathways, and networks can increase our  
67 understanding of underlying pathomechanisms. Prior studies have investigated the differential gene  
68 expression in IBM muscles for both the inflammatory and the degenerative pathology<sup>11-17</sup>. However,  
69 no study has attempted a comprehensive analysis of RNA-seq data combining differential gene  
70 expression, differential exon, and splicing usage along with in-depth analysis of the relation between  
71 dysregulation of coding and regulatory RNAs in IBM muscles.

72 Our study used total RNA extracted from muscle biopsies of IBM patients, of non-myositis RV-  
73 myopathy disease controls, and non-muscle disease controls. We first studied the differential  
74 expression of coding, long non-coding RNAs (lncRNAs), and micro RNAs (miRNAs) and then  
75 evaluated their possible interplay. Additionally, we studied the transcriptome-wide differential exon  
76 and splicing usage. We observed a significant association with genes involved in various calcium-  
77 related pathways and identified disturbed calcium regulation specific to T cells in IBM muscles,  
78 highlighting the relevance of calcium homeostasis for T-cell activity in IBM muscles. In particular,  
79 we identified calcium-induced T lymphocyte apoptosis to be disturbed in IBM muscles.

## 81 **Materials and methods**

### 82 Patients and skeletal muscle biopsies

83 Muscle biopsies (predominantly Tibialis anterior or Vastus lateralis) from 24 Finnish patients  
84 diagnosed with clinically and pathologically defined IBM according to the ENMC criteria<sup>18</sup> were  
85 included. The age of onset was  $60 \pm 11$  years (median  $\pm$  SD), and the age at muscle biopsy was  $70 \pm$   
86  $9$  years. Additionally, muscle biopsies from six patients with genetically diagnosed Tibial muscular  
87 dystrophy (TMD, caused by heterozygous FINmaj mutation the titin gene)<sup>19</sup> were included. In the  
88 TMD cohort, the age of onset was  $49 \pm 11$  years, and age at biopsy  $54 \pm 14$  years. Nine muscle  
89 biopsies from individuals that underwent leg amputation for reasons other than a muscle disease<sup>20</sup>  
90 were also included. These nine biopsies did not show pathologically defined muscle degeneration or  
91 inflammation. Age at sampling for amputees was  $70 \pm 11$  years. All muscle biopsies were snap-frozen  
92 and stored at  $-80$  °C. Muscle biopsies were collected at the Tampere Neuromuscular Research Center,  
93 Tampere University Hospital, Finland.

94 Ethical approval for this study falls under HUS:195/13/03/00/11. Informed consent from the patients  
95 was obtained at the time of sample collection.

### 96 RNA extraction, selection, and library preparation

97 Muscle tissue homogenization steps were performed using SpeedMill PLUS (Analytik Jena AG,  
98 Germany). RNA was extracted with Qiagen RNeasy Plus Universal Mini Kit (Qiagen, Hilden,  
99 Germany) according to the manufacturer's instructions. According to the manufacturer's guidelines,  
100 extracted RNA was treated with Invitrogen TURBO DNase buffer (ThermoFisher Scientific, MA,  
101 USA). RNA was quantified and qualitatively assessed using High Sensitivity RNA ScreenTape  
102 (Agilent Technologies, CA, USA) on Agilent 4200 TapeStation system (Agilent Technologies).

103 Library preparations and sequencing were performed at Oxford Genomics Center, University of  
104 Oxford. For PolyA+ RNA selection, the NEBNext Ultra II Directional RNA Library Prep kit (E7760)  
105 for Illumina (NEB, Beverly, MA, USA) was used to prepare strand-specific RNA-seq libraries.  
106 Libraries were multiplexed and sequenced on HiSeq4000: 75bp paired-end sequencing (Illumina,  
107 CA, USA), and an average of  $\sim 47$  million reads per sample were produced. Samples with enough  
108 RNA were used for library preparation for small RNA ( $< 200$  nt) selection (18 IBM, nine amputees,  
109 and four TMD). NEBNext Small RNA Library Prep Set (E7330) for Illumina was used per the  
110 manufacturer's instructions (NEB). Libraries were multiplexed and sequenced on HiSeq2500: 50bp  
111 single-end sequencing (Illumina), and an average of  $\sim 10$  million reads per sample were produced.

## 112 RNA-seq data pre-processing, QC, and alignment

113 Adapter sequences and low-quality bases were removed with fastp<sup>21</sup>. Trimmed sequences were then  
114 mapped with STAR 2.7.0d<sup>22</sup> (STAR, RRID: SCR\_004463) with index generated from Gencode.v29  
115 human reference (release date 05.2018, based on ENSEMBL GRCh38.p12) and comprehensive gene  
116 annotation (primary assembly) using the STAR two-pass method according to the guidelines from  
117 the ENCODE project for alignment of long RNA (>200 nt) and small RNA (<200 nt) data.

## 118 RNA-seq quantification and differential gene expression analysis

119 Uniquely mapped fragments were summarized and quantified (referred to as counts) by  
120 featureCounts<sup>23</sup> (featureCounts, RRID: SCR\_012919) using Gencode.v29 primary comprehensive  
121 gene annotation which lists 58,780 RNAs including 19,969 protein-coding, 16,066 non-coding and  
122 22,745 other types of RNAs (primary gene expression analysis). Separate quantification of counts for  
123 lncRNA (lncRNA analysis) was done using long non-coding RNA gene annotation from  
124 Gencode.v29 (a subset of the primary annotation). Quantification of counts for miRNAs (miRNA  
125 analysis) in 31 samples was done using miRBase human miRNA annotation (Release 22.1 October  
126 2018)<sup>24</sup>. DGE analysis was performed with DESeq2<sup>25</sup> (v1.26.0) (DESeq2, RRID: SCR\_015687) in  
127 Rstudio (v1.2.5019) (RStudio, RRID: SCR\_000432) based on R (v3.6.3) (R Project for Statistical  
128 Computing, RRID: SCR\_001905). Counts were normalized with variance stabilizing transformation  
129 function within DESeq2. A principal component analysis (PCA) was performed on the gene  
130 expression data of the IBM samples compared to amputee and TMD controls. Further, pairwise  
131 comparisons between cohorts were performed using the Wald test. Log<sub>2</sub> fold changes (LFC) were  
132 shrunk using 'ashr' adaptive shrinkage estimation<sup>26</sup>, and results were generated with default  
133 independent filtering for increasing power. Only genes with LFC values larger than ±1.5 and a  
134 Benjamini-Hochberg adjusted p-value of ≤0.01 were considered further. Genes specifically  
135 dysregulated in IBM muscles were considered for downstream analysis.

## 136 Pathway analysis

137 Ingenuity Pathway Analysis (IPA, QIAGEN Inc.) (Ingenuity Pathway Analysis, RRID:  
138 SCR\_008653) was used for pathway analysis and enrichment analysis of the obtained DGE data.  
139 Using Ingenuity Pathways Knowledge Base (Ingenuity Pathways Knowledge Base, RRID:  
140 SCR\_008117), IPA mapped and annotated genes to the pathways and predicted activation state based  
141 on the direction of changes comparing it with the change in the database.

142

## 143 Differential splicing analysis

144 To investigate differential usage of exons and splicing, independent of the differential gene  
145 expression analysis, we used QoRTS<sup>27</sup> java-based application (v1.3.6) (QoRTs, RRID: SCR\_018665)  
146 to prepare counts from exons and splice junctions (known and novel) from the aligned data.  
147 Downstream analysis of this data was performed using JunctionSeq<sup>28</sup> (v1.16.0) in R. JunctionSeq  
148 results produce a q-value (based on FDR) on gene-level analysis, which considers that one or more  
149 exon/junction in this gene is differentially used. A conservative q-value threshold of 0.01 was used  
150 to select significant observations. IBM-specific differentially expressed genes, and differentially  
151 spliced genes were compared (Fig 1). Statistical over-enrichment analysis for Gene ontology terms  
152 in categories: Molecular function, biological process, and cellular component, was performed on  
153 results obtained from QoRTs/JunctionSeq using clusterProfiler<sup>29</sup> (clusterProfiler, RRID:  
154 SCR\_016884). Gene sets were compared using UpSet plot<sup>30</sup>.

## 155 Data availability

156 Raw counts and normalized DESeq2 counts from polyA+ RNAs and miRNAs are available in GEO  
157 as superseries GSE151758.

## 158 **Results**

### 159 Expression signature is significantly different in IBM muscles as compared to control muscles

160 Fig 1a shows the summarized workflow of the methodology. The PCA shown in Fig 1b explains the  
161 differences between the three cohorts. Pairwise comparisons were performed to reduce the potential  
162 confounding effects of controls, which identified 2,288 and 302 genes specifically up- or down-  
163 regulated in the IBM cohort, respectively (Fig 1c). Non-coding RNA analyses resulted in 497  
164 lncRNAs upregulated, 106 lncRNAs downregulated, 140 miRNAs upregulated, and 126 miRNAs  
165 explicitly downregulated in the IBM cohort compared to control groups. These IBM-specific  
166 dysregulated RNAs were used for downstream pathway analysis using IPA workflow. The top 15  
167 genes dysregulated specifically in IBM muscles, with their functional annotations and normalized  
168 expression in the different cohorts, are shown in Fig 2.

### 169 Pathway analysis

170 We performed IPA workflow analysis on IBM-specific dysregulated genes to better understand the  
171 pathways and the upstream regulators associated with the observed expression dysregulation. Out of  
172 these, 2,588 genes, 596 lncRNAs, and 257 miRNAs mapped to the Ingenuity database. From the

173 primary gene expression analysis, IPA identified 91 pathways as significantly altered. Fig 3a shows  
174 a summary of the IPA results with the top identified pathways.

175 The top upstream regulators in both lncRNA analysis and miRNA analysis are shown in Fig 3c and  
176 3d, respectively. We identified an increased expression of the lncRNA *DNM3OS* (DNM3 antisense  
177 RNA) and *MIAT* (Myocardial infarction associated transcript) from these analyses. IPA suggested  
178 this dysregulation may be due to *JDP2* (Jun Dimerization Protein 2) and *TARDBP* (TAR DNA  
179 Binding Protein), acting as an upstream regulator of *DNM3OS* and *MIAT* respectively (Fig 3c).

#### 180 Dysregulation of calcium-related pathways in IBM muscles

181 IPA identified calcium-induced T lymphocyte apoptosis as one of the most significant pathways  
182 dysregulated in IBM muscles (Fig 3a). Our IBM-specific dataset contained 69 genes with significant  
183 dysregulation out of the 232 genes annotated in this pathway. A part of this pathway, including the  
184 major players, is shown in Fig 4. Another pathway outside the top results identified that 29 genes  
185 (29/208,  $p = 7.05E-03$ ) significantly dysregulated in our dataset are also involved in calcium  
186 signaling. These results prompted us to investigate further for calcium related issues in cellular  
187 signaling, and we found that IPA also detects dysregulation of the following processes, mobilization  
188 of  $Ca^{2+}$  (80 genes), the release of  $Ca^{2+}$  (33 genes), quantity of  $Ca^{2+}$  (51 genes) and flux of  $Ca^{2+}$  (51  
189 genes), as significantly disturbed in IBM muscles (Fig 3b).

#### 190 Altered exon usage and splicing pattern in IBM muscles

191 To explore IBM-specific exon usage, we performed an independent transcriptome-wide differential  
192 splicing analysis in our three cohorts. We obtained a list of 1,271 differentially spliced genes in IBM  
193 from our differential splicing analysis. These transcripts either showed IBM-specific increased usage  
194 of a known junction or a known exon or contained a novel exon-exon junction resulting in an  
195 alternative isoform. To understand the diverse portfolio of mature mRNAs created from pre-mRNAs,  
196 we used gene ontology over-enrichment analysis on these 1,271 differentially spliced genes and  
197 identified the first splicing signature specific to IBM muscles. To understand the different classes  
198 over-represented in these genes, we performed statistical over-enrichment analysis using  
199 clusterProfiler for all three GO categories as seen in Fig. 5 a,b,c. Our analysis showed an enrichment  
200 of genes involved in the structure and organization of actin filaments assembly in IBM muscles and,  
201 interestingly, proteins involved in mRNA processing and metabolism.

202 We then compared the list of differentially spliced genes with differentially expressed genes in our  
203 analysis and found an overlap of 79 genes (Fig. 1d). Next, we wanted to observe the overlap between

204 six different sets of genes, namely IBM specific differentially spliced genes, calcium-induced T  
205 Lymphocyte apoptosis, Mobilization of Ca<sup>2+</sup>, Flux of Ca<sup>2+</sup>, Quantity of Ca<sup>2+</sup>, and Release of Ca<sup>2+</sup>  
206 (Fig. 5d). We observed 10 genes to be associated with calcium-related processes; *HLA-DPA1*, *HLA-*  
207 *DPB1*, and *HLA-DQB1* are associated with calcium-induced T Lymphocyte apoptosis, *ANXA1* is  
208 associated with mobilization, flux, and release of Ca<sup>2+</sup>, *CCL4* is associated with mobilization, flux,  
209 and quantity of Ca<sup>2+</sup>, *GRK3* and *RARRES2* are associated with mobilization, *SH3KBP1* with flux, and  
210 *ITGAM* with the quantity of Ca<sup>2+</sup>. In particular, one specific differentially spliced gene, *LCK*, is part  
211 of all six sets.

212 Fig 6a shows the gene expression of *LCK* in three cohorts, with expression in IBM muscles being  
213 significantly higher than the others ( $\log_2FC = +2.86$ ,  $padj=3.50E-11$ , ranking = 355/2590).  
214 Additionally, Fig 6b shows the differential splicing pattern observed in *LCK* in all three groups. The  
215 highlighted E016 corresponds to an alternative exon (chr1:32274818-32274992, GRCh38).

## 216 Discussion

217 In this study, we aimed to identify a more detailed IBM-specific molecular signature, using different  
218 RNA-seq based methods that can help us explore the inflammatory and degenerative parts in depth.  
219 Antigen-driven T-cell cytotoxicity is the most reproducible and plausible part of the complex  
220 molecular pathomechanism in IBM. However, it remains unknown what antigen drives this IBM-  
221 specific immune cascade.

222 As part of the RV pathology, accumulated proteins or the unfolded protein response have been  
223 hypothesized to prompt an immune reaction<sup>8</sup>. A recent unbiased proteomics study dissected these  
224 RVs in IBM<sup>31</sup>. Interestingly, the protein encoded by one of our top differentially expressed genes,  
225 *MYL4*, is also detected in the RVs in IBM along with *ANXA1*, which is both differentially expressed  
226 and differentially spliced in IBM muscles. In our study design, we considered TMD, another RV  
227 muscle disease but without immune involvement, as a control to understand if there are any RV-  
228 specific antigens in IBM muscles. Additionally, using age matched histopathologically normal  
229 muscles from amputees, we aimed to understand if general inflammatory signatures can be replicated  
230 and studied in more detail using additional methods such as non-coding RNAs and differential  
231 splicing studies. Consequently, our strong study design and robust methodology helped us replicate  
232 findings from previous studies<sup>11-17</sup> and identify essentially new calcium-related issues in IBM  
233 muscles and their link with the altered T-cell cytotoxicity in IBM muscle fibers.

234 We found that several genes contributing to calcium homeostasis are differentially expressed in IBM  
235 muscles resulting in dysregulation of several critical pathways, specifically, calcium-induced T



236 lymphocyte apoptosis and related Nur77 signaling.  $\text{Ca}^{2+}$  is a universal second messenger in T cells,  
237 and it is known to regulate proliferation and differentiation of T cells and T-cell effector functions<sup>32</sup>.  
238 The complexity and duration of  $\text{Ca}^{2+}$  signals and resultant cytoskeletal rearrangements determine the  
239 fate of T cells in response to an antigen<sup>33</sup>. On one hand, a short-term increase in intracellular  $\text{Ca}^{2+}$   
240 concentration results in the cytolytic activity of T cells; on the other hand, prolonged elevation results  
241 in proliferation, differentiation, and maturation of naïve T cells into Th1, Th2, and Th17 subtypes and  
242 the production of cytokines<sup>32</sup>.

243  $\text{Ca}^{2+}$  signaling is known to optimize the interaction between T cells and antigen-presenting cells<sup>33</sup>.  
244 The binding of antigen/MHC complexes ( $\text{CD8}^+$ -MHC class I/ $\text{CD4}^+$ -MHC class II) to T-cell receptors  
245 (TCR) activates Src-family protein tyrosine kinases, e.g., LCK and FYN at the cytoplasmic side of  
246 the TCR/CD3 complex. Additionally, activation of ZAP-70, a tyrosine kinase associate protein,  
247 results in the phosphorylation and activation of the intracellular enzyme phospholipase C- $\gamma$ 1 (PLC-  
248  $\gamma$ 1)<sup>32,33</sup>. PLC- $\gamma$ 1 hydrolyses phosphatidylinositol 4,5-biphosphate (PIP2) to produce two other second  
249 messengers, inositol 1,4,5-triphosphate (IP3) and diacylglycerol (DAG). IP3 binds to its receptor  
250 (IP3R) on the endoplasmic reticulum (ER) membrane to promote rapid release of  $\text{Ca}^{2+}$  from ER to  
251 the cytosol<sup>32</sup>. However, this release of  $\text{Ca}^{2+}$  is insufficient for antigen-derived T-cell fate but results  
252 in depletion of intracellular  $\text{Ca}^{2+}$  triggering a rapid influx of  $\text{Ca}^{2+}$  through activation and opening of  
253  $\text{Ca}^{2+}$  release- $\text{Ca}^{2+}$  activated channels (CRAC) on the plasma membrane formed by different  
254 STIM1/ORAI1 combinations<sup>34</sup>. The duration of  $\text{Ca}^{2+}$  influx is vital for activating the calcineurin-  
255 dependent nuclear factor activate T cells (NFAT) transcription pathway<sup>32</sup>. In the cytoplasm,  
256 calcineurin removes excess phosphate residues from the N terminus of NFAT, promoting its entry  
257 into the nucleus. Disruptions in NFAT signaling can cause several phenotypes, including  
258 cardiovascular, musculoskeletal, and immunological diseases<sup>35</sup>. Meanwhile, DAG, another  
259 secondary messenger, activates protein kinase C (PKC), which in turn activates the nuclear factor  
260 kappa B (NF $\kappa$ B). The duration and complexity of  $\text{Ca}^{2+}$  signals drive the NFAT/NF $\kappa$ B signaling and  
261 determine downstream T-cell activation.

262 The genes in the NR4A family (NR4A1/Nur77, NR4A2/Nurr1, NR4A3/Nor1) act as critical  
263 molecular switches in cell survival and inflammation. Human *NR4A1* encodes for a homolog of a  
264 mouse protein called Nur77, a zinc transcription factor expressed as an early gene in T cells upon  
265 antigen-TCR interaction. In addition to being a transcriptional activator, Nur77 has an apoptotic role  
266 in T regulatory fate<sup>36</sup> and other non-genomic proapoptotic functions via mitochondrial interactions  
267 with Bcl-2<sup>37</sup>. T cells deficient in Nur77 have been shown to have high proliferation, enhanced T-cell  
268 activation, and increased susceptibility for T-cell-mediated inflammatory diseases<sup>38</sup>. The expression

269 of Nur77 is Ca<sup>2+</sup> dependent and is controlled by the myocyte enhancer factor 2 (MEF2) transcription  
270 factor<sup>39</sup>, whose DNA-binding and transcriptional activity is enhanced by Calcineurin. Another  
271 calcium-dependent transcription factor, CABIN1, acts as a transcriptional repressor of MEF2, thus  
272 keeping the Nur77 promoter silent in the absence of a TCR signal<sup>40</sup>. The interaction between CABIN1  
273 and calcineurin is influenced by intracellular Ca<sup>2+</sup> and PKC activation, resulting in  
274 hyperphosphorylation of CABIN1 and its subsequent transcription repressing activity. An increase in  
275 intracellular Ca<sup>2+</sup> concentration activates the interaction of the calmodulin family of genes (CALM)  
276 with CABIN1, triggering the dissociation of MEF2 from Cabin and MEF2 to become  
277 transcriptionally active<sup>41</sup>. In the nucleus, NFAT interacts with MEF2 and enhances its transcriptional  
278 activity by recruiting the co-activator p300 for the transcription of Nur77.

279 In our dataset, 69 genes mapping to the calcium-induced T Lymphocyte apoptosis and 72 genes  
280 mapping the Nur77 signaling in T Lymphocytes are differentially expressed in IBM muscles. As seen  
281 in Figure 4, several essential genes like *ZAP70*, *LCK*, different subunits of Protein Kinase C, and  
282 *ATP2A1* which encodes for SERCA, are significantly changed in IBM muscles. Additionally, we also  
283 observed genes associated with mobilization of Ca<sup>2+</sup>, release of Ca<sup>2+</sup>, quantity of Ca<sup>2+</sup> and flux of  
284 Ca<sup>2+</sup> as significantly dysregulated in IBM muscles, indicating a possible widespread disturbance with  
285 the handling of calcium entry and release in cells. In T cells, especially, this disturbance could  
286 dramatically impact their activation, differentiation, and most likely, the regulation of T-cell apoptosis  
287 will be disturbed.

288 Apoptosis in T cells is necessary to resolve their inflammatory activity, and defective or delayed  
289 apoptosis may contribute to the pathogenesis of inflammatory diseases<sup>42</sup>. In this scenario, loss of  
290 apoptotic control could be one mechanism explaining the lack of immune-suppressive therapeutic  
291 effect in IBM.

292 The diversity of the skeletal muscle proteome is, among others, dependent on the diversity of exon  
293 usage in pre-mRNAs<sup>43</sup>. From our transcriptome-wide splicing analysis within the differentially  
294 expressed genes, we identified 79 genes, out of which ten are associated with different calcium-  
295 related functions. Amongst these, *LCK* is a T lymphocyte-specific protein tyrosine kinase involved  
296 in downstream events of antigen–TCR interaction. *LCK/p56* is essential in transducing signals  
297 leading to apoptotic cell death in mature T cells<sup>44</sup>, and its activity is tightly regulated to protect against  
298 hyperactivation of T cells and autoimmunity, thus maintaining T-cell homeostasis<sup>45</sup>. Moreover, *LCK*  
299 also selectively influences the flux and release of calcium in cells<sup>46</sup>. In our analysis, *LCK* is both  
300 differentially expressed and differentially spliced in IBM muscles. Disturbed T-cell apoptosis and the

301 dysregulation of LCK in IBM muscles provide novel insights into the molecular mechanisms of IBM.  
302 Considering the crucial regulatory activity of LCK, it might be a potential therapeutic target for IBM  
303 patients.

304 We also observe dysregulation of several non-coding RNAs in our study. Previously, Hamann and  
305 colleagues have discussed lncRNAs in the context of IBM<sup>13</sup>. The benefits of our study design,  
306 especially the homogenous molecular pathology and the larger sample size, let us dig deeper into the  
307 dysregulation of lncRNAs specific to IBM muscles. We identified specific JDP2 (DNA binding  
308 transcription factor) and TARDBP/TDP-43 (DNA and RNA binding protein), may have altered  
309 regulator activity since their downstream non-coding partners (*DNM3OS* and *MIAT*, respectively) are  
310 significantly overexpressed IBM muscles. Additionally, both these proteins are specific to RNA  
311 polymerase II (RNA Pol II), facilitating transcription and pre-mRNA maturation. Alteration in RNA  
312 or DNA binding proteins (expression or localization) associated with the activity of the spliceosome  
313 machinery can directly affect the downstream events. Since TDP-43 is accumulated in RVs, one  
314 possibility is that the unavailability of TDP-43 can affect its transcription and splicing activities. The  
315 normal expression of *TARDBP* we observe in IBM patients is expected and is in coherence with the  
316 previous reports<sup>47</sup>. In inherited muscle diseases, damaging variants in the disease-associated gene can  
317 result in mislocalization and accumulation of mutant protein in the muscle fibers. Previous studies  
318 have reported rare exonic variants in genes, including *VCP* and *SQSTM1* in IBM<sup>48, 49</sup>. However, in  
319 our cohort of IBM patients, there were no rare exonic *TARDBP*, *VCP*, or *SQSTM1* variants<sup>6</sup> that could  
320 suggest a possible association with abnormal protein turnover and accumulation/aggregation.  
321 Therefore, further evidence to suggest the pathogenic role of variants in such genes and their  
322 downstream effect on pathological protein accumulation in IBM is still missing. However, the  
323 potential downside of TDP-43 not being available for its traditional roles, such as effective splicing,  
324 because of the aggregation is noteworthy. Further evidence of possible dysregulation of splicing in  
325 IBM muscles comes from our differential splicing results where proteins involved in mRNA  
326 processing, transcription, and regulation are enriched, suggesting that additional studies are needed  
327 to understand the possible impact of dysregulated mRNA processing in IBM muscles.

328 Previously, Pinal-Fernandez and colleagues observed that calcium-induced T lymphocyte apoptosis  
329 was a significant IBM-specific dysregulated pathway in their extensive analysis of different  
330 inflammatory myopathies but did not comment further on the possible importance<sup>17</sup>. Additionally,  
331 using a smaller sample size, Amici and colleagues identified calcium signaling as one of the  
332 significant disturbed pathways in IBM muscles and hypothesized its potential major role<sup>14</sup>.  
333 Furthermore, previous gene expression studies in IBM have analyzed data primarily from

334 microarrays<sup>11, 12, 15</sup>. Only recently paired-end reads RNA-seq have been used in IBM studies<sup>13, 14, 16,</sup>  
335 <sup>17</sup>. While microarray-based analyses are comparable for differential expression studies, RNA-seq  
336 based methodologies are superior for in-depth transcriptome analysis. In our study design, we used  
337 matched muscle biopsies and state-of-the-art RNA-seq analysis tools. Our analyses show novel  
338 molecular events in IBM muscles which increase our understanding of IBM and provide valuable  
339 additions to improve the therapeutic interventions considering the disturbed calcium homeostasis,  
340 dysregulation of LCK, and associated deregulation of apoptotic control of T cells in IBM muscles.

## 341 **Acknowledgments**

342 The authors would like to thank the patients and their families. We thank the Oxford Genomics Centre  
343 at the Wellcome Centre for Human Genetics (funded by Wellcome Trust grant reference  
344 203141/Z/16/Z) for the generation and initial processing of the sequencing data. We would like to  
345 thank CSC – IT Center for Science, Finland, for its computational resources. We thank Merja  
346 Soininen, Talha Qureshi and Eini Penkkimäki for their technical assistance. We would like to thank  
347 Peter-Bram 't Hoen for his critical review of this manuscript.

## 348 **Funding**

349 This work was supported by the Folkhälsan Research Foundation, Doctoral program in Integrative  
350 Life Science (ILS) and Doctoral school in Health Sciences (DSHealth), University of Helsinki (MJ),  
351 the Päivikki and Sakari Sohlberg Foundation (MJ), the Biomedicum Helsinki Foundation (MJ),  
352 Finska läkaresällskapet (BU/MJ), the Finnish Medical Foundation (JP), the Paulo foundation (MS),  
353 the Jane and Aatos Erkko Foundation (PH) and the Sigrid Jusélius Foundation (BU).

## 354 **Author Contributions**

355 MJ: Conceptualization of the study, funding acquisition, data analysis and curation, methodology,  
356 project administration, visualization, writing the original draft, review, and editing of the  
357 manuscript.

358 AV: data analysis, methodology, writing the original draft.

359 JP: Patient samples and data collection, writing the original draft.

360 MJ: Patient samples and data collection, review, and editing of the manuscript.

361 PH.J.: Conceptualization of the methodology, review, and editing of the manuscript.

362 JS: Data analysis, review, and editing of the manuscript.

363 SH: Patient samples and data collection, review, and editing of the manuscript.

364 MS: Conceptualization of the study and methodology, review and editing of the manuscript.

365 PH: Funding acquisition, project administration, and review and editing of the manuscript.

366 BU.: Conceptualization of the study, funding acquisition, supervision, project administration,  
367 review, and editing of the manuscript.

368 **Conflicts of interest**

369 The authors report no conflicts of interest.

## 370 **References**

- 371 1. Ikenaga C, Kubota A, Kadoya M, et al. Clinicopathologic features of myositis patients  
372 with CD8-MHC-1 complex pathology. *Neurology* 2017;89:1060-1068.
- 373 2. Hanna MG, Badrising UA, Benveniste O, et al. Safety and efficacy of intravenous  
374 bimagrumab in inclusion body myositis (RESILIENT): a randomised, double-blind, placebo-controlled  
375 phase 2b trial. *Lancet Neurol* 2019;18:834-844.
- 376 3. Cai H, Yabe I, Sato K, et al. Clinical, pathological, and genetic mutation analysis of  
377 sporadic inclusion body myositis in Japanese people. *J Neurol* 2012;259:1913-1922.
- 378 4. Amato AA, Shebert RT. Inclusion body myositis in twins. *Neurology* 1998;51:598-600.
- 379 5. Askanas V, Engel WK. Sporadic inclusion-body myositis: a proposed key pathogenetic  
380 role of the abnormalities of the ubiquitin-proteasome system, and protein misfolding and  
381 aggregation. *Acta Myol* 2005;24:17-24.
- 382 6. Johari M, Arumilli M, Palmio J, et al. Association study reveals novel risk loci for  
383 sporadic inclusion body myositis. *Eur J Neurol* 2017;24:572-577.
- 384 7. Rothwell S, Chinoy H, Lamb JA, et al. Focused HLA analysis in Caucasians with myositis  
385 identifies significant associations with autoantibody subgroups. *Annals of the Rheumatic Diseases*  
386 2019;78:996-1002.
- 387 8. Askanas V, Engel WK. Sporadic inclusion-body myositis and hereditary inclusion-body  
388 myopathies: current concepts of diagnosis and pathogenesis. *Curr Opin Rheumatol* 1998;10:530-  
389 542.
- 390 9. Greenberg SA. Theories of the pathogenesis of inclusion body myositis. *Curr*  
391 *Rheumatol Rep* 2010;12:221-228.
- 392 10. Hiniker A, Daniels BH, Margeta M. T-Cell-Mediated Inflammatory Myopathies in HIV-  
393 Positive Individuals: A Histologic Study of 19 Cases. *J Neuropathol Exp Neurol* 2016;75:239-245.
- 394 11. Greenberg SA, Sanoudou D, Haslett JN, et al. Molecular profiles of inflammatory  
395 myopathies. *Neurology* 2002;59:1170-1182.
- 396 12. Eisenberg I, Eran A, Nishino I, et al. Distinctive patterns of microRNA expression in  
397 primary muscular disorders. *Proc Natl Acad Sci U S A* 2007;104:17016-17021.
- 398 13. Hamann PD, Roux BT, Heward JA, et al. Transcriptional profiling identifies differential  
399 expression of long non-coding RNAs in Jo-1 associated and inclusion body myositis. *Sci Rep*  
400 2017;7:8024.
- 401 14. Amici DR, Pinal-Fernandez I, Mazala DA, et al. Calcium dysregulation, functional  
402 calpainopathy, and endoplasmic reticulum stress in sporadic inclusion body myositis. *Acta*  
403 *Neuropathol Commun* 2017;5:24.
- 404 15. Greenberg SA, Pinkus JL, Kong SW, Baecher-Allan C, Amato AA, Dorfman DM. Highly  
405 differentiated cytotoxic T cells in inclusion body myositis. *Brain* 2019;142:2590-2604.
- 406 16. Pinal-Fernandez I, Casal-Dominguez M, Derfoul A, et al. Identification of distinctive  
407 interferon gene signatures in different types of myositis. *Neurology* 2019;93:e1193-e1204.
- 408 17. Pinal-Fernandez I, Casal-Dominguez M, Derfoul A, et al. Machine learning algorithms  
409 reveal unique gene expression profiles in muscle biopsies from patients with different types of  
410 myositis. *Ann Rheum Dis* 2020;79:1234-1242.
- 411 18. Rose MR, Group EIW. 188th ENMC International Workshop: Inclusion Body Myositis,  
412 2-4 December 2011, Naarden, The Netherlands. *Neuromuscul Disord* 2013;23:1044-1055.
- 413 19. Hackman P, Vihola A, Haravuori H, et al. Tibial muscular dystrophy is a titinopathy  
414 caused by mutations in TTN, the gene encoding the giant skeletal-muscle protein titin. *Am J Hum*  
415 *Genet* 2002;71:492-500.

- 416 20. Huovinen S, Penttila S, Somervuo P, et al. Differential isoform expression and selective  
417 muscle involvement in muscular dystrophies. *Am J Pathol* 2015;185:2833-2842.
- 418 21. Chen S, Zhou Y, Chen Y, Gu J. fastp: an ultra-fast all-in-one FASTQ preprocessor.  
419 *Bioinformatics* 2018;34:i884-i890.
- 420 22. Dobin A, Davis CA, Schlesinger F, et al. STAR: ultrafast universal RNA-seq aligner.  
421 *Bioinformatics* 2013;29:15-21.
- 422 23. Liao Y, Smyth GK, Shi W. featureCounts: an efficient general purpose program for  
423 assigning sequence reads to genomic features. *Bioinformatics* 2014;30:923-930.
- 424 24. Griffiths-Jones S. The microRNA Registry. *Nucleic Acids Res* 2004;32:D109-111.
- 425 25. Love MI, Huber W, Anders S. Moderated estimation of fold change and dispersion for  
426 RNA-seq data with DESeq2. *Genome Biol* 2014;15:550.
- 427 26. Stephens M. False discovery rates: a new deal. *Biostatistics* 2016;18:275-294.
- 428 27. Hartley SW, Mullikin JC. QoRTs: a comprehensive toolset for quality control and data  
429 processing of RNA-Seq experiments. *BMC Bioinformatics* 2015;16:224.
- 430 28. Hartley SW, Mullikin JC. Detection and visualization of differential splicing in RNA-Seq  
431 data with JunctionSeq. *Nucleic Acids Res* 2016;44:e127.
- 432 29. Yu G, Wang LG, Han Y, He QY. clusterProfiler: an R package for comparing biological  
433 themes among gene clusters. *OMICS* 2012;16:284-287.
- 434 30. Lex A, Gehlenborg N, Strobel H, Vuillemot R, Pfister H. UpSet: Visualization of  
435 Intersecting Sets. *IEEE Transactions on Visualization and Computer Graphics* 2014;20:1983-1992.
- 436 31. Güttsches A-K, Brady S, Krause K, et al. Proteomics of rimmed vacuoles define new risk  
437 allele in inclusion body myositis. *Annals of neurology* 2017;81:227-239.
- 438 32. Joseph N, Reicher B, Barda-Saad M. The calcium feedback loop and T cell activation:  
439 how cytoskeleton networks control intracellular calcium flux. *Biochim Biophys Acta* 2014;1838:557-  
440 568.
- 441 33. Lewis RS. Calcium signaling mechanisms in T lymphocytes. *Annu Rev Immunol*  
442 2001;19:497-521.
- 443 34. Qu B, Al-Ansary D, Kummerow C, Hoth M, Schwarz EC. ORAI-mediated calcium influx  
444 in T cell proliferation, apoptosis and tolerance. *Cell Calcium* 2011;50:261-269.
- 445 35. Crabtree GR, Olson EN. NFAT signaling: choreographing the social lives of cells. *Cell*  
446 2002;109 Suppl:S67-79.
- 447 36. Calnan BJ, Szychowski S, Chan FK, Cado D, Winoto A. A role for the orphan steroid  
448 receptor Nur77 in apoptosis accompanying antigen-induced negative selection. *Immunity*  
449 1995;3:273-282.
- 450 37. Thompson J, Winoto A. During negative selection, Nur77 family proteins translocate  
451 to mitochondria where they associate with Bcl-2 and expose its proapoptotic BH3 domain. *J Exp*  
452 *Med* 2008;205:1029-1036.
- 453 38. Liebmann M, Hucke S, Koch K, et al. Nur77 serves as a molecular brake of the  
454 metabolic switch during T cell activation to restrict autoimmunity. *Proceedings of the National*  
455 *Academy of Sciences* 2018;115:E8017-E8026.
- 456 39. Youn HD, Chatila TA, Liu JO. Integration of calcineurin and MEF2 signals by the  
457 coactivator p300 during T-cell apoptosis. *The EMBO journal* 2000;19:4323-4331.
- 458 40. Youn HD, Liu JO. Cabin1 represses MEF2-dependent Nur77 expression and T cell  
459 apoptosis by controlling association of histone deacetylases and acetylases with MEF2. *Immunity*  
460 2000;13:85-94.
- 461 41. Palmer E. Negative selection--clearing out the bad apples from the T-cell repertoire.  
462 *Nat Rev Immunol* 2003;3:383-391.

- 463 42. Raza K, Scheel-Toellner D, Lee CY, et al. Synovial fluid leukocyte apoptosis is inhibited  
464 in patients with very early rheumatoid arthritis. *Arthritis Res Ther* 2006;8:R120.
- 465 43. Nakka K, Ghigna C, Gabellini D, Dilworth FJ. Diversification of the muscle proteome  
466 through alternative splicing. *Skeletal Muscle* 2018;8:8.
- 467 44. Yu X-Z, Levin SD, Madrenas J, Anasetti C. Lck Is Required for Activation-Induced T Cell  
468 Death after TCR Ligation with Partial Agonists. *The Journal of Immunology* 2004;172:1437-1443.
- 469 45. McNeill L, Salmond RJ, Cooper JC, et al. The differential regulation of Lck kinase  
470 phosphorylation sites by CD45 is critical for T cell receptor signaling responses. *Immunity*  
471 2007;27:425-437.
- 472 46. Thompson JL, Shuttleworth TJ. A plasma membrane-targeted cytosolic domain of  
473 STIM1 selectively activates ARC channels, an arachidonate-regulated store-independent Orai  
474 channel. *Channels (Austin)* 2012;6:370-378.
- 475 47. Cortese A, Plagnol V, Brady S, et al. Widespread RNA metabolism impairment in  
476 sporadic inclusion body myositis TDP43-proteinopathy. *Neurobiol Aging* 2014;35:1491-1498.
- 477 48. Wehl CC, Baloh RH, Lee Y, et al. Targeted sequencing and identification of genetic  
478 variants in sporadic inclusion body myositis. *Neuromuscul Disord* 2015;25:289-296.
- 479 49. Gang Q, Bettencourt C, Machado PM, et al. Rare variants in SQSTM1 and VCP genes  
480 and risk of sporadic inclusion body myositis. *Neurobiol Aging* 2016;47:218 e211-218 e219.

481



## 482 **Figures and tables**

483 Figure 1: a) Workflow and methodology used in this study. b) Principal component analysis of gene  
484 expression results showing the pairwise comparison between IBM, control TMD and control amputee  
485 populations. c) IBM-specific differentially expressed genes were determined by comparing IBM  
486 cases with amputee and TMD controls. d) Comparison between IBM specific differentially expressed  
487 genes (cyan) and IBM specific differentially spliced genes (magenta).

488 Figure 2: a) Top 15 differentially expressed genes specific to IBM muscles. Log<sub>2</sub> fold change  
489 (log<sub>2</sub>FC) of IBM versus amputees calculated by DEseq2 after shrinkage estimations. '+'/'-' sign  
490 denotes the direction of change, i.e., positive log<sub>2</sub>FC values indicate overexpressed genes in IBM  
491 muscles and negative log<sub>2</sub>FC values indicate underexpressed genes in IBM muscles. The p-value of  
492 significance and adjusted p-value using the Benjamini-Hochberg corrections and associated GO  
493 terms are shown for each gene. Genes marked with \* are also observed as significantly dysregulated  
494 in Hamann et al.<sup>13</sup> b) Normalized gene expression in the different cohorts is presented as boxplots.  
495 Median and quartile values are shown with whiskers reaching up to 1.5 times the interquartile range.  
496 Individual expression levels are shown as jitter points. The raincloud plots illustrate the distribution  
497 of data in each cohort. The scaled Y-axis shows log normalized counts.

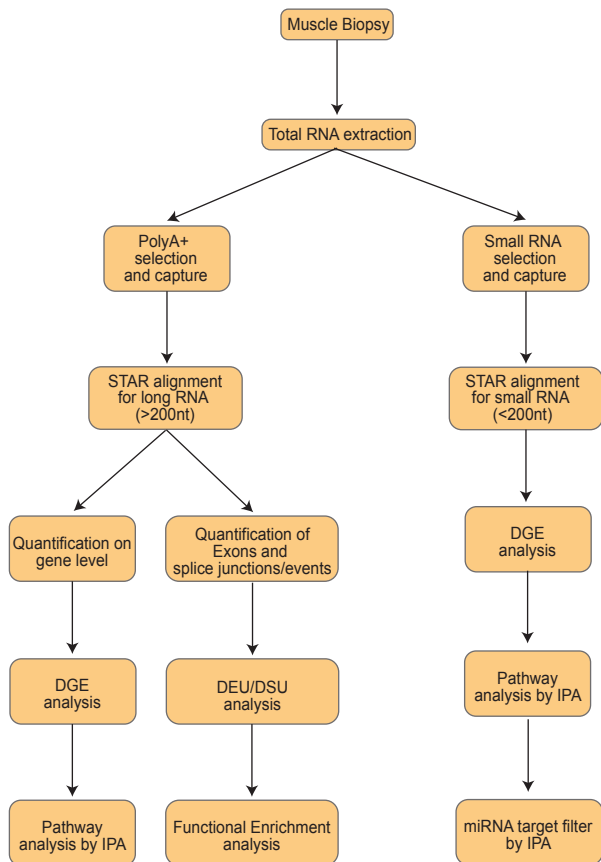
498 Figure 3: a) Top 10 dysregulated canonical pathways identified by IPA. The significance of the  
499 identified pathway is shown with a p-value and the number of differentially expressed genes observed  
500 in the IBM-specific dataset compared to the number of genes present in the database for each  
501 pathway. b) In cell signaling processes, different pathways associated with calcium homeostasis are  
502 shown along with their p-value and a prediction state. c) in the long non-coding RNA analysis,  
503 upstream binding partners are shown along with their target lncRNA. A p-value and associated GO  
504 terms are shown. d) in the miRNA analysis, upstream binding partners are shown along with their  
505 target miRNA. A p-value and associated GO terms are shown.

506 Figure 4: The calcium-induced T lymphocyte apoptosis pathway with gene expression changes  
507 observed in IBM compared to controls. Created with BioRender.com

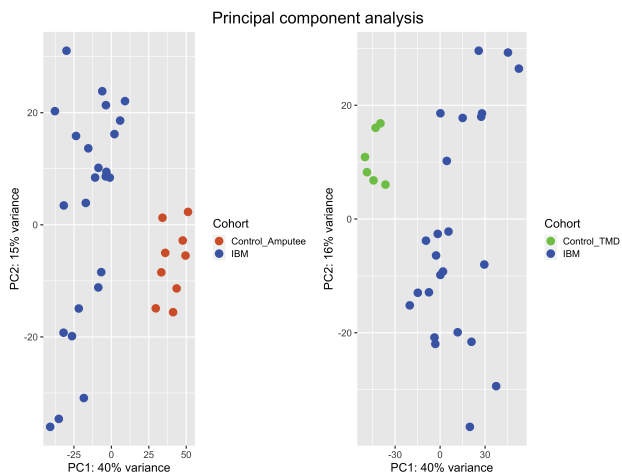
508 Figure 5. Statistical over-representation tests were performed on a list of differentially spliced RNAs,  
509 using clusterProfiler for a) Biological Processes, b) Cellular component, and c) Molecular function.  
510 d) An UpSet plot is shown comparing six different sets, namely, IBM specific differentially spliced  
511 (1,271 genes), mobilization of Ca<sup>2+</sup> (80 genes), calcium-induced T lymphocyte apoptosis (69 genes),  
512 the flux of Ca<sup>2+</sup> (51 genes), quantity of Ca<sup>2+</sup> (51 genes), and release of Ca<sup>2+</sup> (33 genes). Dots and lines  
513 represent subsets of different lists. The horizontal bar graph (wine color) represents the size of each  
514 set, while the vertical histogram (black) represents the number of RNAs in each subset. The 10 RNAs  
515 that are both differentially expressed and differentially spliced are shown with a red circle with their  
516 gene names (black).

517 Figure 6. a) Normalized LCK expression in the different cohorts (as explained in Fig 2b). b) Altered  
518 isoform expression of *LCK* using JunctionSeq showing estimated normalized mean read-pair count  
519 for each exon and splice junctions in the different cohorts (left) as well as for the whole *LCK* gene  
520 (right). The significantly alternatively spliced feature, E016 (pink), corresponds to chr1:32274818-  
521 32274992 (GRCh38). The alternative *LCK* transcripts used in the JunctionSeq analysis are shown  
522 below with their corresponding ENSEMBL identifiers.

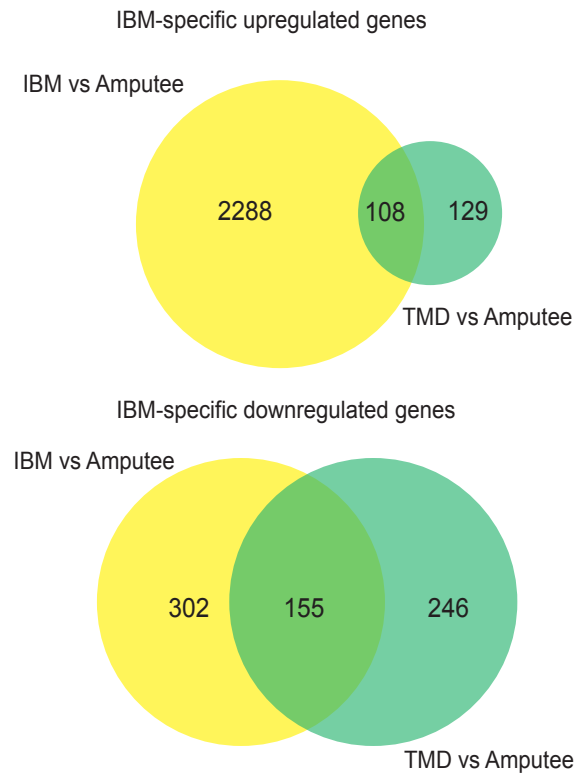
a



b



c



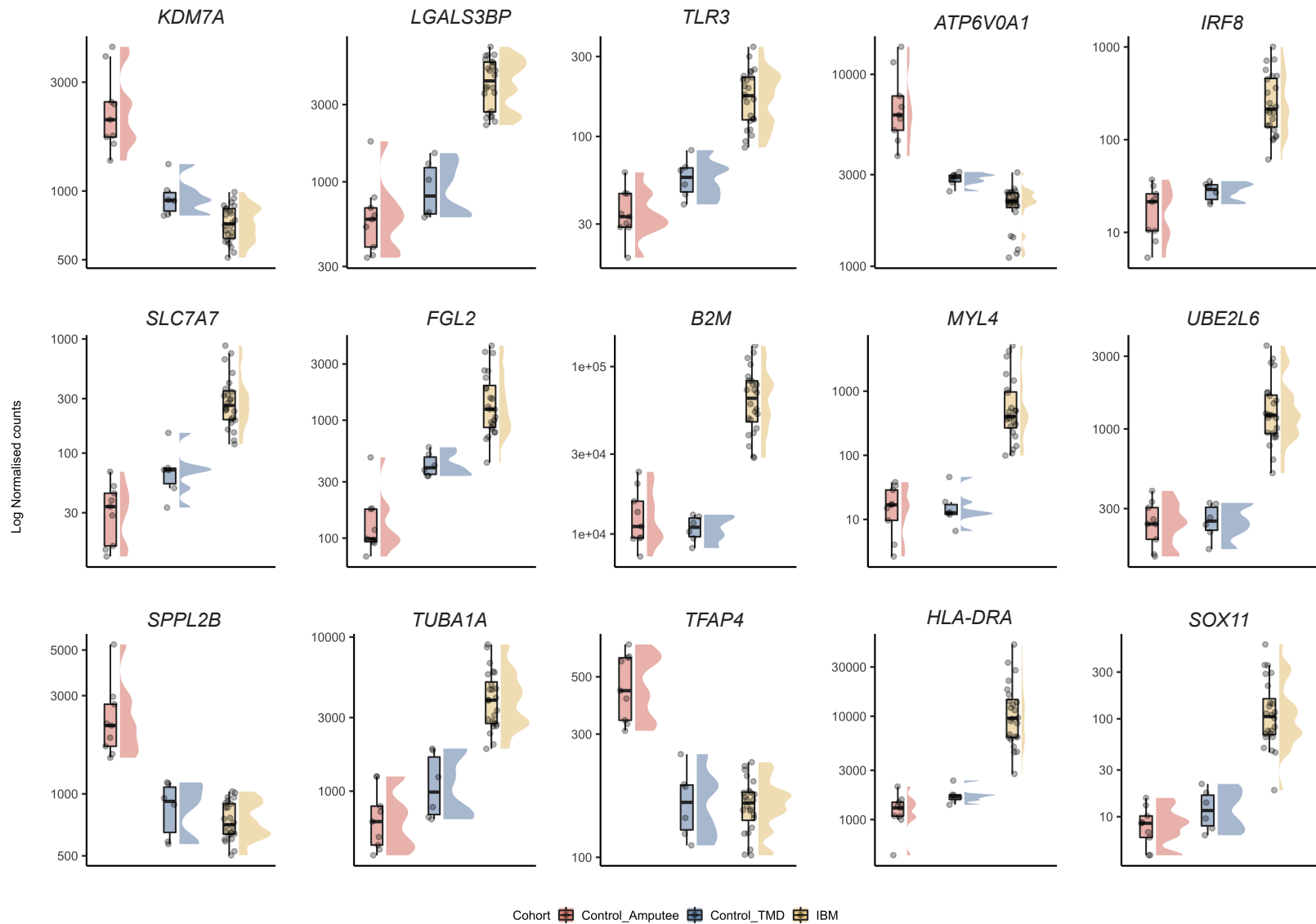
d



a

Symbol	Mean count	log2FC	pvalue	padj	GO terms
<i>KDM7A</i>	1147.06	-1.69	4.07E-32	2.39E-28	Iron ion binding and oxidoreductase activity
<i>LGALS3BP*</i>	2922.28	2.59	5.91E-31	2.89E-27	Scavenger receptor activity
<i>TLR3</i>	128.42	2.29	3.98E-28	1.30E-24	Regulation of dendritic cell cytokine production
<i>ATP6V0A1</i>	3393.79	-1.76	3.01E-27	8.83E-24	ATPase binding and proton-transporting ATPase activity
<i>IRF8*</i>	199.90	3.89	4.66E-27	1.24E-23	DNA-binding transcription factor activity, RNA polymerase II-specific
<i>SLC7A7</i>	216.91	3.16	2.08E-26	5.09E-23	Amino acid transmembrane transporter activity
<i>FGL2</i>	1102.10	3.27	3.14E-26	6.58E-23	T cell activation via T cell receptor contact with antigen bound to MHC molecule on antigen presenting cell
<i>B2M*</i>	46381.30	2.29	4.71E-26	9.22E-23	Positive regulation of T cell mediated cytotoxicity
<i>MYL4*</i>	610.22	5.44	5.92E-26	1.09E-22	Actin monomer binding, Calcium ion binding
<i>UBE2L6*</i>	986.03	2.47	1.86E-25	3.04E-22	Ubiquitin-protein transferase activity
<i>SPPL2B</i>	1161.90	-1.66	2.99E-25	4.39E-22	Protein homodimerization activity
<i>TUBA1A*</i>	2951.15	2.50	4.36E-25	5.81E-22	GTPase activity, structural molecule activity
<i>TFAP4</i>	234.41	-1.52	4.32E-25	5.81E-22	Transcription regulatory region sequence-specific DNA binding
<i>HLA-DRA</i>	8658.66	3.25	7.29E-25	9.00E-22	Antigen processing and presentation of endogenous peptide antigen via MHC class II
<i>SOX11</i>	96.02	4.03	1.97E-24	2.23E-21	DNA-binding transcription factor activity, RNA polymerase II-specific

b



a

Ingenuity Canonical Pathways	Number of genes in dataset / Number of genes in database		
	p-value		z-score
<b>Dendritic Cell Maturation</b>	5.72E-31	106/357	7.02
<b>T Cell Receptor Signaling</b>	2.30E-25	97/355	8.981
<b>T Cell Exhaustion Signaling Pathway</b>	3.12E-25	94/338	2.191
<b>Cdc42 Signaling</b>	7.63E-24	88/315	3.3
<b>iCOS-iCOSL Signaling in T Helper Cells</b>	4.10E-23	81/280	5.099
<b>CD28 Signaling in T Helper Cells</b>	1.13E-22	82/290	3.578
<b>OX40 Signaling Pathway</b>	4.03E-21	68/222	1.633
<b>Calcium-induced T Lymphocyte Apoptosis</b>	1.29E-20	69/232	4.359
<b>Nur77 Signaling in T Lymphocytes</b>	3.07E-20	72/253	3.162
<b>Role of NFAT in Regulation of the Immune Response</b>	4.57E-19	87/360	5.916

b

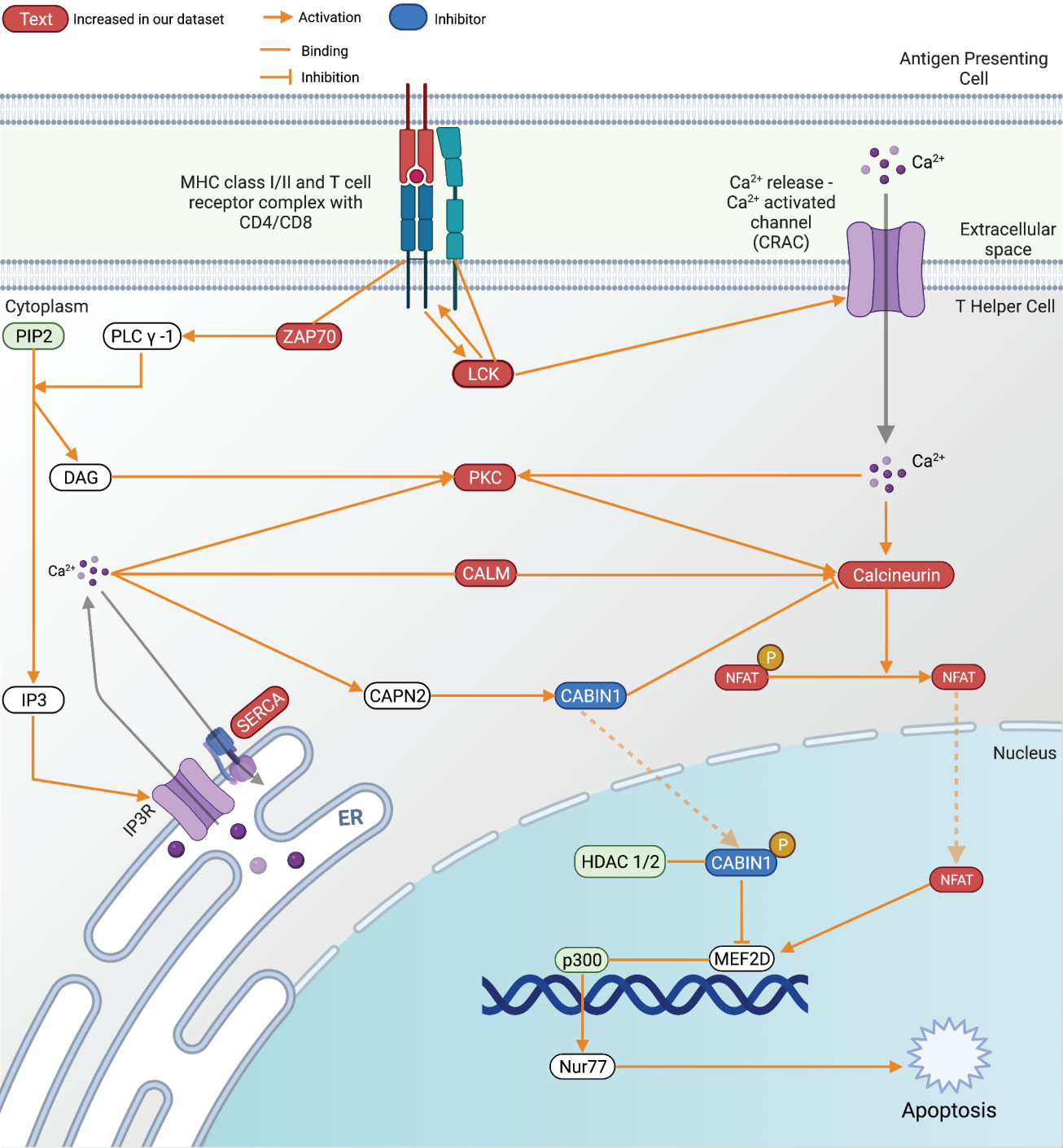
Functional annotations	p-value	Predicted activation state
<b>Mobilization of Ca<sup>2+</sup></b>	5.04E-26	Increased
<b>Flux of Ca<sup>2+</sup></b>	4.68E-13	Increased
<b>Quantity of Ca<sup>2+</sup></b>	4.34E-09	Increased
<b>Release of Ca<sup>2+</sup></b>	5.00E-09	Increased

c

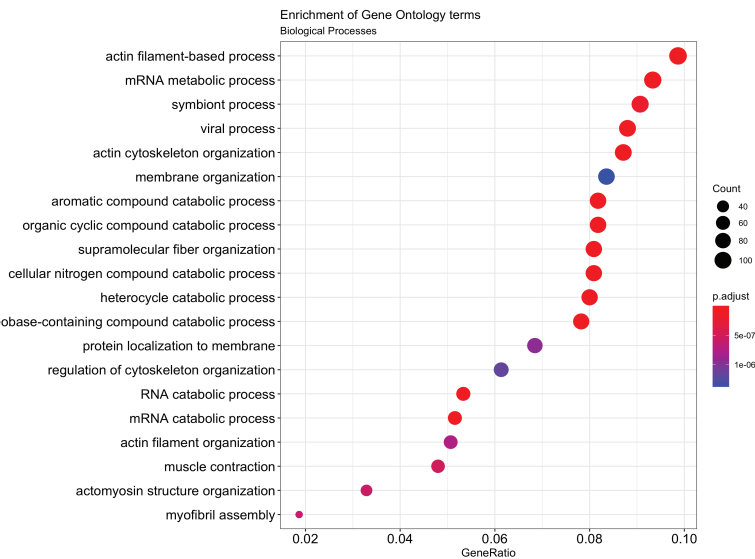
Upstream regulator	Target molecule in dataset	p-value	GO terms and annotations
<b><i>JDP2</i></b>	<i>DNM3OS</i>	4.10E-03	DNA-binding transcription factor activity, RNA polymerase II-specific
<b>miR-338-3p</b>	<i>NR2F1-AS1</i>	4.10E-03	Negative regulation of gene expression; negative regulation of IL-6 production; negative regulation of cytokine production involved in inflammatory response
<b>miR-150-5p</b>	<i>MIAT</i>	4.10E-03	mRNA binding involved in posttranscriptional gene silencing
<b><i>TARDBP</i></b>	<i>MIAT</i>	2.03E-02	RNA polymerase II cis-regulatory region sequence-specific DNA binding
<b>mir-150</b>	<i>MIAT</i>	2.63E-02	mRNA binding involved in posttranscriptional gene silencing
<b><i>PGF</i></b>	<i>DNM3OS</i>	3.43E-02	Protein binding, signal transduction
<b><i>FUS</i></b>	<i>RMRP</i>	3.43E-02	mRNA binding, mRNA stabilization
<b><i>DDX58</i></b>	<i>EGOT</i>	4.61E-02	double-stranded RNA binding

d

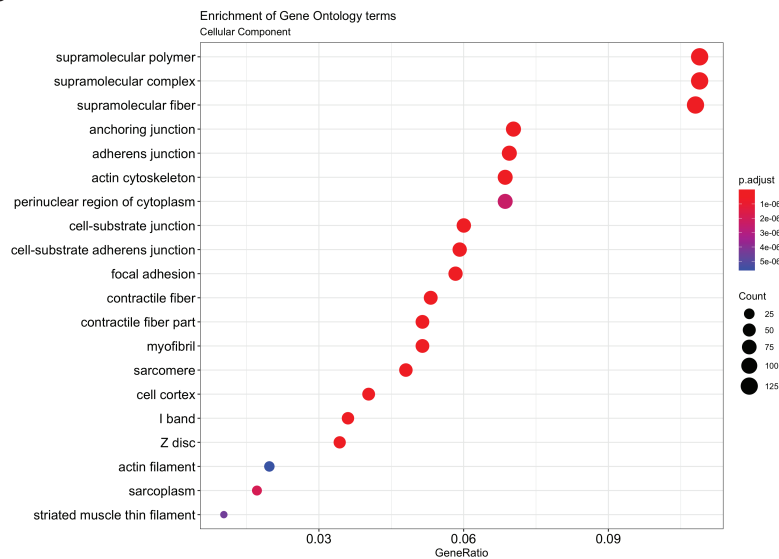
Upstream regulator	p-value	GO terms and annotations
<b><i>AGO2</i></b>	7.89E-23	RNA polymerase II complex binding
<b><i>SSB</i></b>	4.74E-19	RNA binding
<b><i>TP53</i></b>	7.59E-09	Transcription regulatory region sequence-specific DNA binding
<b>RNA polymerase III</b>	4.09E-06	Synthesis of small RNA, RNA polymerase activity



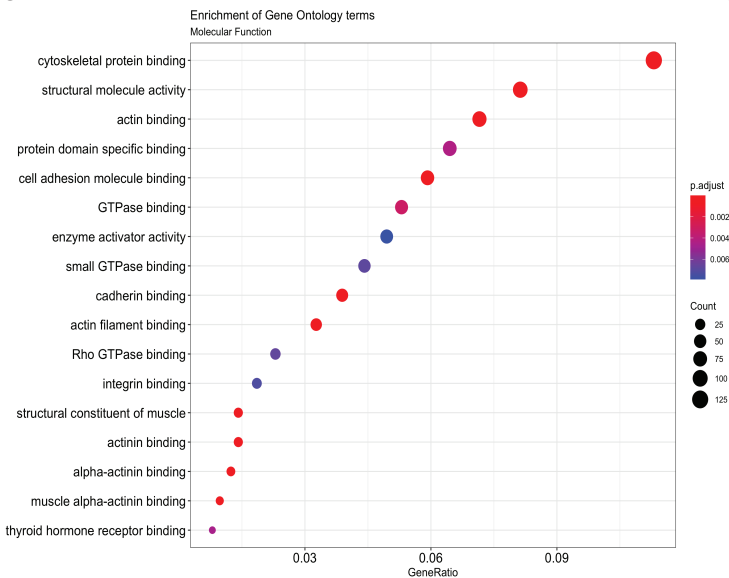
a



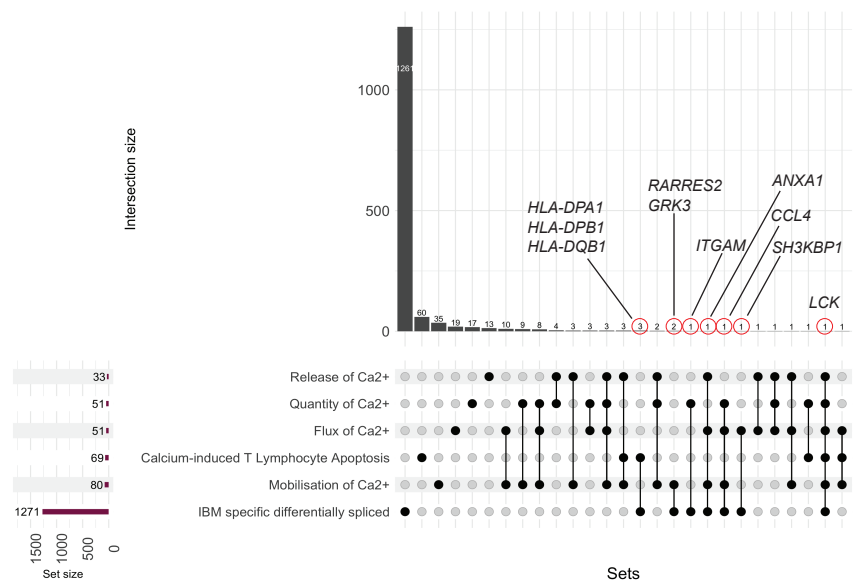
b



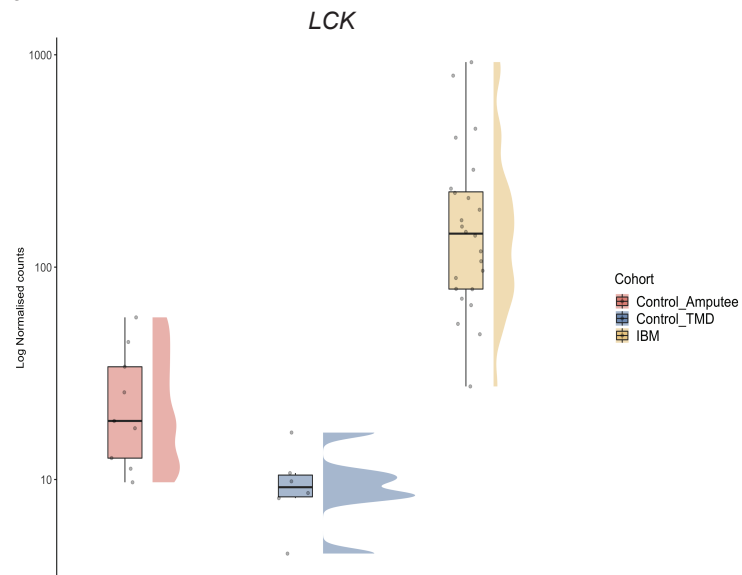
c



d



a



b

